

Machine Learning Holographic Mapping by Neural Network Renormalization Group

Hong-Ye Hu,¹ Shuo-Hui Li,^{2,3} Lei Wang,^{2,4,5} and Yi-Zhuang You^{1,*}

¹*Department of Physics, University of California at San Diego, La Jolla, CA 92093, USA*

²*Institute of Physics, Chinese Academy of Sciences, Beijing 100190, China*

³*University of Chinese Academy of Sciences, Beijing 100049, China*

⁴*CAS Center for Excellence in Topological Quantum Computation,
University of Chinese Academy of Sciences, Beijing 100190, China*

⁵*Songshan Lake Materials Laboratory, Dongguan, Guangdong 523808, China*
(Dated: May 15, 2022)

We develop the neural network renormalization group as a model-independent approach to design general forms of exact holographic mapping (EHM) for interacting field theories. The EHM constitutes a bijection that maps a conformal field theory (CFT) on the holographic boundary to a gapped field theory in the holographic bulk, aiming to reduce the mutual information in the bulk field. We design a flow-based hierarchical deep generative neural network as a variational realization of the EHM. Given the CFT action, we first train the neural network to find the optimal EHM by assuming the bulk field as independent random variables. We then use the trained EHM to map the CFT back to a bulk effective action, from which the holographic bulk geometry can be measured from the residual mutual information in the bulk field. We apply this approach to the complex ϕ^4 theory in two-dimensional Euclidian spacetime, and show that the holographic bulk matches the three-dimensional hyperbolic geometry.

PACS numbers: 05.10.Cc, 11.25.Hf, 04.62.+v

Introduction— The holographic duality, also known as the anti-de-Sitter space and conformal field theory correspondence (AdS/CFT) [1–4], is a duality between a CFT on a flat boundary and a gravitational theory in the AdS bulk with one higher dimension. It is intrinsically related to the renormalization group (RG) flow [5–11] of the boundary quantum field theory, since the dilation transformation, as a part of the conformal group, naturally corresponds to the coarse-graining procedure in the RG flow. The extra dimension emergent in the holographic bulk can be interpreted as the RG scale. In the traditional real-space RG [12], the coarse-graining procedure decimates irrelevant degrees of freedom along the RG flow, therefore the RG transformation is irreversible due to the information loss. However, if the decimated degrees of freedom are collected and hosted in the bulk, the RG transformation can constitute a *bijective* map between the degrees of freedom on the CFT boundary and the degrees of freedom in the AdS bulk. Such mappings, generated by information-preserving RG transforms, are called exact holographic mappings (EHM) [13–15], which were first formulated for free fermion CFT. Similar idea was also implemented by multiscale entanglement renormalization ansatz (MERA) [16, 17] as a hierarchical quantum circuit, as well as many of its generalizations [18–26].

Under the EHM, the boundary features of different scales are mapped to different depths in the bulk, and vice versa. The field variable deep in the bulk represents the overall or infrared (IR) feature, while the variable close to the boundary controls the detailed or ultraviolet (UV) feature. Such a hierarchical arrangement of information is often observed in deep neural networks, partic-

ularly in convolutional neural networks (CNN) [?]. The similarity between renormalization group and deep learning has been discussed in several works [27–31]. Deep learning techniques have also been applied to construct the optimal RG scheme [32, 33] and to uncover the holographic geometry [34–36]. In this work, we further explore the possibility of constructing the EHM for interacting quantum field theories using deep learning. The construction will enable us to establish the holographic duality on the field theory level and to probe the emergent dual geometry by measuring the field correlation function in the holographic bulk.

Neural-RG Method— We focus on the quantum field theories of scalar fields $\phi(x)$ in flat Euclidean spacetime. The coordinate $x = (x^1, x^2, \dots)$ can be more than one dimension in general. The action functional $S[\phi(x)]$ of the field theory determines the probability density of a field configuration $\phi(x)$ following the Boltzmann distribution

$$Q[\phi(x)] = e^{-S[\phi(x)]}/Z. \quad (1)$$

We train a deep neural network to learn the optimal RG scheme for the field theory. The key is to realize that renormalization and generation are inverses of each other. They constitute the forward and backward maps of an EHM. Each step of an information-preserving RG transforms the fine-grained field into the coarse-grained field together with the holographic bulk field that contains the detail information needed to invert the mapping. The steps can be organized in a hierarchical network as shown in Fig. 1(a). If we run the mapping in the reversed direction, the network will organize the bulk field $\zeta(x, z)$ to generate the original field $\phi(x)$ on the holographic bound-

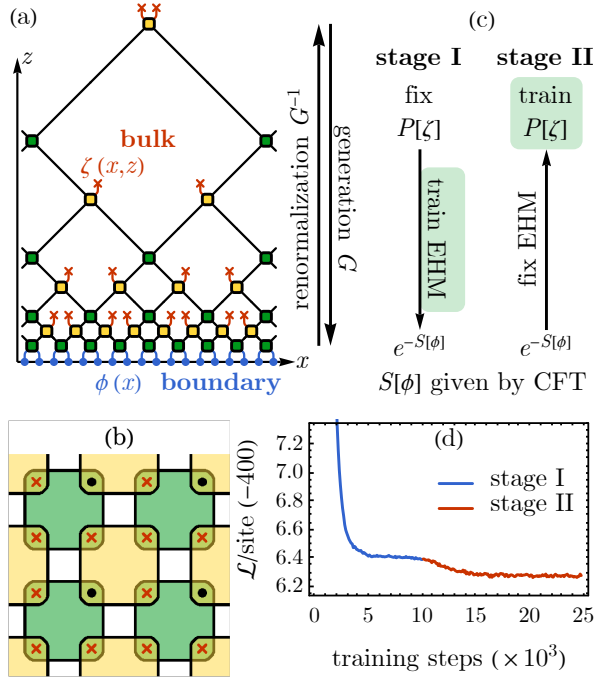


FIG. 1. (a) Side view of the neural-RG network. x is the spatial dimension(s) and z corresponds to the RG scale. There are two types of blocks: disentangers (dark green) and decimators (light yellow). The network forms an EHM between the boundary variables (blue dots) and the bulk variables (red crosses). (b) Top view of one RG layer in the network. Disentangers and decimators interweave in the spacetime (taking two-dimensional spacetime for example). Each decimator pushes the coarse-grained variable (black dot) to the higher layer and leaves the decimated variables (red crosses) in the holographic bulk. (c) The training contains two stages. In the first stage, we fix the prior distribution $P[\zeta]$ to be uncorrelated Gaussian and train the EHM G to bring it to the Boltzmann distribution of the CFT. In the second stage, we learn the prior distribution with the trained EHM held fixed. (d) The behavior of the loss function \mathcal{L} in the two training stages.

ary (i.e. the visible layer),

$$\phi(x) = G[\zeta(x, z)], \quad (2)$$

so the reverse RG flow simply corresponds to a deep generative model G . Developing a good RG scheme of a field theory is equivalent to training a good hierarchical generative model that generates the boundary field $\phi(x)$ following the designated Boltzmann distribution $Q[\phi] \propto e^{-S[\phi]}$ as much as possible.

Another important objective of RG is to progressively distill the relevant features in the field configuration and decimate irrelevant features. Since the bulk field $\zeta(x, z)$ hosts the decimated features, it encodes the information that we choose to forget about under the RG flow, which should appear to us as independent random noise. Therefore we propose that the information theoretical goal of

the RG (or the EHM more precisely) is to minimize the mutual information among the bulk field fluctuations, such that the EHM effectively decouples the field theory at each scale progressively. The “minimal bulk mutual information” principle we proposed here is in spirit consistent with the “maximal real-space mutual information” principle proposed recently in Ref. 33 and 37, which aims at maximizing the mutual information between the coarse-grained field and the fine-grained field in the surrounding environment, such that minimal amount of information is pushed to the bulk field (see Supplementary Material A for the relation between these two principles). In the simplest setup, we can hard code the minimal bulk mutual information by assigning the bulk field to follow the uncorrelated Gaussian distribution,

$$P[\zeta(x, z)] = \mathcal{N}[\zeta(x, z); \mathbf{0}, \mathbf{1}]. \quad (3)$$

Then the generative model serves as a bijection $\phi = G[\zeta]$ that deforms the trivial Gaussian prior distribution $P[\zeta]$ in the bulk to a non-trivial posterior distribution $P_\partial[\phi]$ on the boundary,

$$P_\partial[\phi] = P[\zeta] \left| \det \left(\frac{\delta G[\zeta]}{\delta \zeta} \right) \right|^{-1}. \quad (4)$$

Then the problem of constructing the optimal EHM boils down to training the optimal generative model G to minimize the Kullback-Leibler (KL) divergence between the model distribution $P_\partial[\phi]$ and the target distribution $Q[\phi]$, given the bulk field as a trivial random source,

$$\mathcal{L} = \text{KL}(P_\partial[\phi] || Q[\phi]). \quad (5)$$

By minimizing the loss function \mathcal{L} , the generative model learns how to efficiently organize random variables in the holographic bulk to generate the field configurations on the holographic boundary that match the given quantum field theory. This is an unsupervised learning problem: no labels are provided to the field configurations. The only input we need is a black box function that can evaluate the action $S[\phi(x)]$ for any given field configuration $\phi(x)$. At this stage, the goal is first to train the EHM to disentangle the boundary field theory, so the prior distribution $P[\zeta]$ should be fixed uncorrelated to guide the training. We call it the training stage I in Fig. 1(c).

We design the generative model G as a bijective deep neural network following the architecture of the neural-RG proposed by Ref. 32. Its structure resembles the MERA network [16] as depicted in Fig. 1(a). Each RG step contains a layer of disentangler blocks (like CNN convolutional layer) to resolve local correlations, and a layer of decimator blocks (like CNN pooling layer) to separate the renormalized and decimated variables. For the case that the spacetime dimension is two on the boundary, we can overlay decimators on top of disentangers as in Fig. 1(b). Both the disentangler and the decimator are made of three bijective layers: a linear scaling layer,

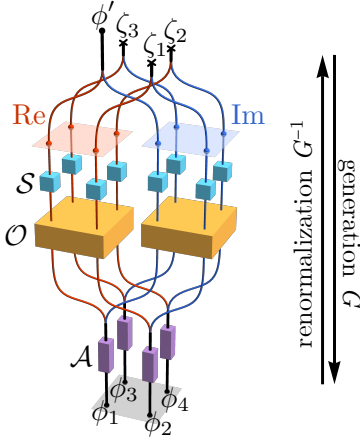


FIG. 2. Neural network architecture within a decimator block (the disentangler block shares the same architecture). Starting from the renormalized variable ϕ' and the bulk noise $\zeta_{1,2,3}$ as complex variables, the Re and Im channels are first separated, then S applies the scaling separately to the four variables within each channel and O implements the $O(4)$ transformation that mixes the four variables together. S and O are identical for Re and Im channels to preserve the $U(1)$ symmetry. Then the channels merge into complex variables followed by element wise non-linear activation describe by an invertible $U(1)$ -symmetric map $\phi_i \mapsto (\phi_i/|\phi_i|) \sinh |\phi_i|$.

an orthogonal transformation layer and an invertible non-linear activation layer, as arranged in Fig. 2. The bijector parameters are subject to training. The Jacobian matrix of these transformations can be easily calculated. After each decimator, only one renormalized variable flows to the next RG layer. The other decimated variables are positioned into the bulk as little crosses. The entire network constitutes an EHM between the original boundary field $\phi(x)$ and the dual field $\zeta(x, z)$ in the holographic bulk.

After learning the optimal EHM, we can use it to push the boundary field back into the bulk and investigate the effective bulk theory induced by the boundary CFT. In general, the bulk field will not remain uncorrelated anymore, because the machine-learned EHM cannot fully resolve all correlations in the original CFT. This is partially limited by the capacity and trainability of the neural network, but more fundamentally due to the lack of a *classical* gravitational dual description for generic CFT. The residual correlation (mutual information) contained in the bulk field fluctuation can be used to probe the holographic bulk geometry. Because the bulk field excitations are typically massive and can not propagate far, we expect the mutual information between the bulk field variables at two different points to decay exponentially with their geodesic distance in the bulk. Following this idea, suppose $\zeta_i = \zeta(x_i, z_i)$ and $\zeta_j = \zeta(x_j, z_j)$ are two bulk field variables, then their distance $d(\zeta_i : \zeta_j)$ can be inferred from their mutual information $I(\zeta_i : \zeta_j)$ as

follows

$$d(\zeta_i : \zeta_j) = -\xi \ln \frac{I(\zeta_i : \zeta_j)}{I_0}, \quad (6)$$

where the correlation length ξ and the information unit I_0 are global fitting parameters. The mutual information is defined with respect to the joint distribution of the bulk field $Q_{\text{bulk}}[\zeta] = Q[\phi] |\det(\delta G^{-1}[\phi]/\delta \phi)|^{-1}$, given the boundary field Boltzmann distribution $Q[\phi] \propto e^{-S[\phi]}$ and the EHM functional G . However, it is difficult to estimate the mutual information in this way, because sampling ϕ from the CFT is generally challenging. Instead of calculating $Q_{\text{bulk}}[\zeta]$ directly, we can train another probability model $P[\zeta]$ to approximate $Q_{\text{bulk}}[\zeta]$. This constitutes the training stage II in Fig. 1(c), where the loss function \mathcal{L} is still the KL divergence in Eq. (5), but the key difference that we freeze the network parameters in the generative model G and train the prior distribution $P[\zeta]$. We will elaborate our strategy to parameterize $P[\zeta]$ based on a concrete example in the following.

Before we dive into details, let us comment on the general behavior of the stage II training. As demonstrated in Fig. 1(d), the loss function will typically drop further in this stage as $P[\zeta]$ gets improved to capture the residual bulk field correlation. So the goal of the stage II training is to distill an effective theory for the bulk field ζ , which can be used to evaluate mutual information $I(\zeta_i, \zeta_j)$ and to measure bulk geodesic distance $d(\zeta_i, \zeta_j)$ following the proposal of Eq. (6). Combining both stages, we can investigate the emergent holographic bulk geometry in correspondence to the boundary CFT. One may wonder why not training the generative model G and bulk field distribution $P[\zeta]$ jointly. This is because there is a trade-off between these two objectives. For example, one can weaken the disentangers in G and push more correlation to the bulk field distribution $P[\zeta]$. Such trade-off will undermine our objective of minimizing bulk mutual information in training a good EHM, therefore the two training stages should be separated, or should be at least assigned very different learning rates separately. In the following, we will apply the two-stage neural-RG approach to study the holographic dual of a Luttinger liquid CFT.

EHM for Complex ϕ^4 Model— We first apply the neural-RG method to construct the optimal EHM for a two-dimensional complex ϕ^4 theory in the conformal phase. Consider the lattice field theory described by the Euclidean action

$$S[\phi] = -t \sum_{\langle ij \rangle} \phi_i^* \phi_j + \sum_i (\mu |\phi_i|^2 + \lambda |\phi_i|^4), \quad (7)$$

where $\phi_i \in \mathbb{C}$ is a complex scalar field defined on each site i of a square lattice and $\langle ij \rangle$ denotes the summation over all nearest neighbor sites. We choose $\mu = -200 + 2t$ and $\lambda = 25$ to create a deep Mexican hat potential that pins the complex field to a circle $\phi_i = \sqrt{\rho} e^{i\theta_i}$ of radius

$\sqrt{\rho} = 2$. In this way, the field theory falls back to the XY-model $S_{XY} = -\frac{1}{T} \sum_{\langle ij \rangle} \cos(\theta_i - \theta_j)$ with an effective temperature $T = (\rho t)^{-1}$. By tuning the temperature T , the model exhibits two phases: the low- T algebraic liquid phase with a power-law correlation $\langle \phi_i^* \phi_j \rangle \sim |x_i - x_j|^{-\alpha}$ and the high- T disordered phase with a short-range correlation. The two phases are separated by the Kosterlitz-Thouless (KT) transition. We focus on the algebraic liquid phase, described by a Luttinger liquid CFT.

We start with a 32×32 square lattice as the holographic boundary and build up the neural-RG network. The disentangler and decimator blocks are interweaving 2×2 squares, as illustrated in Fig. 1(b), such that the network has five layers in total. Since the boundary field theory has an internal U(1) symmetry (under which $\phi_i \rightarrow e^{i\alpha} \phi_i$), the bijectors in the neural network are designed to respect the U(1) symmetry (see Fig. 2), such that the bulk field also preserves the U(1) symmetry. The network can be trained by sampling from the bulk $\zeta \sim P[\zeta]$, generating the boundary field $\phi = G[\zeta]$ to evaluate the loss function \mathcal{L} in Eq. (5), back-propagating its gradient with respect to the network parameters, and updating the parameters by gradient descent.

We train several neural networks at different temperatures T . After training, the neural network could generate configurations of the boundary field ϕ from the bulk uncorrelated Gaussian field ζ efficiently. To test how well these generative models work, we measured the order parameter $\langle \phi \rangle$ and the correlation function $C(|x_i - x_j|) = \langle \phi_i^* \phi_j \rangle$ on the field configurations generated by the neural networks. Although the order parameter $\langle \phi \rangle$ is expected to vanish in the thermodynamic limit, for our finite-size system, it is not vanishing and can exhibit a crossover around the KT transition, as shown in Fig. 3(a). The cross over temperature $T \simeq 0.9$ agrees with the previous Monte Carlo study [38–40] of the KT transition temperature $T_{KT} = 0.8929$ in the two-dimensional XY model. In the algebraic liquid phase, the correlation function fits well to the power-law decay, as shown in Fig. 3(b). The statistics of ϕ_i in one generated sample shows the “spontaneous symmetry breaking” behavior in Fig. 3(c) due to the finite-size effect, although accumulating over multiple samples will restore the U(1) symmetry. In the disordered phase, the correlation decays exponentially as shown in Fig. 3(d), and the U(1) symmetry is present in every single sample in Fig. 3(e).

From these tests, we can conclude that the neural network has learned to generate field configurations $\phi(x)$ that can reproduce the main physics of the complex ϕ^4 theory. If we run the generative model reversely as $\zeta = G^{-1}[\phi]$, it will map the strongly correlated ϕ field (described by a CFT) to an almost uncorrelated ζ field in the holographic bulk, therefore the trained generative model G provides a good EHM for the ϕ^4 theory.

Probing the Holographic Geometry— To probe the holographic bulk geometry, we initiate the training stage

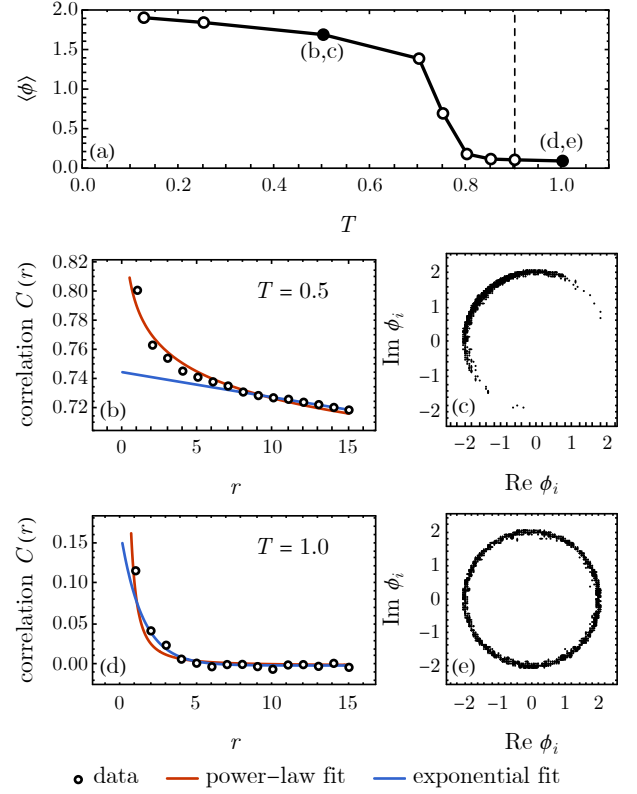


FIG. 3. Performance of the trained EHM for the complex ϕ^4 theory. (a) Order parameter $\langle \phi \rangle$ v.s. temperature T . Different models are trained separately at different temperature. For finite-sized system, $\langle \phi \rangle$ crosses over to zero around the KT transition. (b) Correlation function $\langle \phi_i^* \phi_j \rangle$ scaling and (c) ϕ_i distribution in the algebraic liquid phase. (d) Correlation function $\langle \phi_i^* \phi_j \rangle$ scaling and (e) ϕ_i distribution in the disordered phase.

II to learn the bulk field distribution $P[\zeta]$. It is natural to consider an energy-based model $P[\zeta] \propto e^{-S_{\text{eff}}[\zeta]}$ in terms of an effective action $S_{\text{eff}}[\zeta]$ of the bulk field. In the continuum limit, the action is expected to take the general form of a scalar field on a curved spacetime background \mathcal{M} equipped with the metric tensor $g^{\mu\nu}$,

$$S_{\text{eff}}[\zeta] = \int_{\mathcal{M}} \frac{1}{2} (g^{\mu\nu} \partial_\mu \zeta^* \partial_\nu \zeta + m^2 |\zeta|^2 + u |\zeta|^4 + \dots). \quad (8)$$

Our starting point of assuming the bulk field to follow the uncorrelated Gaussian distribution corresponds to the limit of $m \rightarrow \infty$ in Eq. (8). We expect that the actual bulk effective theory would not deviate from that limit too far, i.e. the bulk field is still very massive. In that case, the higher order interaction terms are irrelevant, and the bulk field could be controlled by a Gaussian model. Based on this assumption, we use a correlated Gaussian distribution with the kernel matrix K to model the bulk field fluctuation on top of the network

$$P[\zeta] = \frac{1}{\sqrt{\det(2\pi K^{-1})}} \exp\left(-\frac{1}{2} \zeta_i^* K_{ij} \zeta_j\right), \quad (9)$$

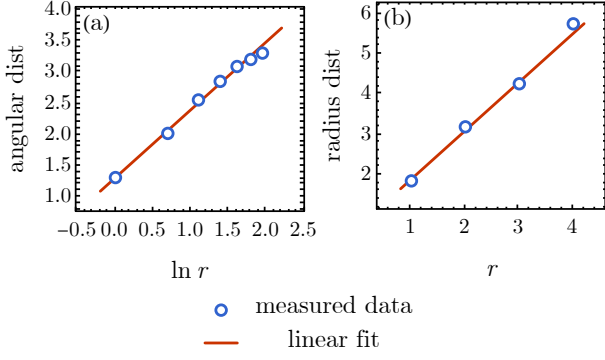


FIG. 4. Distance scaling in radius and angular direction.

where ζ_i denotes the bulk field on the node i in the neural network. The kernel matrix K is carefully designed to ensure positivity and bulk locality (see Supplemental Material B for more details). We use the reparametrization trick [41] to sample the correlated Gaussian, such that the gradient signal can backpropagate to the kernel K . As we relax the Gaussian kernel K for training, we can see that the loss function will continue to drop in the stage II, as shown in Fig. 1(d). This indicates that the Gaussian model is learning to capture the residual bulk field correlation (at least partially), such that the overall performance of generation gets improved. This stage of training can be considered as fixing a background geometry and try to learn the effective theory for the matter field fluctuation in the holographic bulk.

After training, we obtain the optimal kernel matrix K . The mutual information $I(\zeta_i : \zeta_j)$ can be evaluated with respect to the correlated Gaussian distribution $P[\zeta]$,

$$I(\zeta_i : \zeta_j) = -\frac{1}{2} \ln \left(1 - \frac{\langle \zeta_i^* \zeta_j \rangle}{\langle \zeta_i^* \zeta_i \rangle \langle \zeta_j^* \zeta_j \rangle} \right), \quad (10)$$

where the bulk correlation $\langle \zeta_i^* \zeta_j \rangle = (K^{-1})_{ij}$ is simply given by the inverse of the kernel matrix K . Then we can measure the holographic distance $d(\zeta_i : \zeta_j)$ between any pair of bulk variables ζ_i and ζ_j following Eq. (6). To probe the bulk geometry, we further define the distance between two decimators A and B to be the average distance between all pairs of bulk variables separately associated to them,

$$D(A : B) = \text{avg}_{\zeta_i \in A, \zeta_j \in B} d(\zeta_i : \zeta_j). \quad (11)$$

Each decimator is labeled by three coordinates (x^1, x^2, z) , where $x = (x^1, x^2)$ denotes its center position projected to the holographic boundary and $z = 2^l$ is related to its layer depth l (ascending from UV to IR). We found that the measured distance function follows the scaling behavior

$$\begin{aligned} D(x^1, x^2, z : x^1 + r, x^2, z) &\propto \ln r, \\ D(x^1, x^2, z : x^1, x^2, z + r) &\propto r, \end{aligned} \quad (12)$$

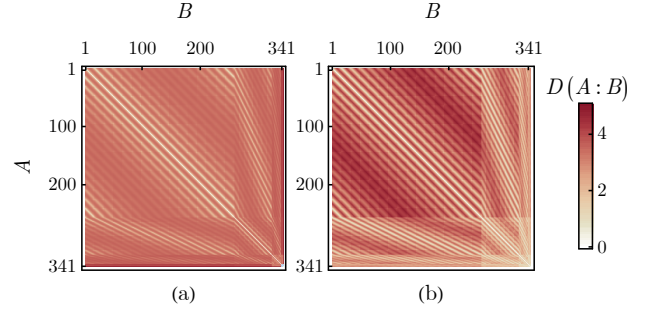


FIG. 5. Comparison between (a) the measured distance matrix from the bulk field mutual information and (b) the ideal distance matrix of a hyperbolic space. The overall feature of the measured distance matrix matches that of the hyperbolic space. Each block in the distance matrix corresponds to one RG layer, from UV (the largest block) to IR (the smallest block). Structures in diagonal (or off-diagonal) blocks represent intra-layer (or inter-layer) spacetime connections.

as demonstrated in Fig. 4. These scaling behaviors agree with the geometry of a three-dimensional hyperbolic space H^3 , which corresponds to the AdS_3 spacetime under the Wick rotation of the time dimension (see Supplementary Material C for details about hyperbolic space). We can arrange all the decimators lexicographically and assign each decimator with a unique index A . The distance $D(A : B)$ for all decimators A and B can be arranged into a matrix. As shown in Fig. 5, the measured distance matrix matches well with the ideal distance matrix calculated in a hyperbolic space. This indicates that the emergent bulk geometry is indeed hyperbolic at the classical level. Our result demonstrates that the holographic dual of the Luttinger liquid CFT can be approximated by (generally interacting) massive scalar fields on AdS_3 background geometry. It is also possible to go beyond the Gaussian model to investigate the interaction among the bulk scalar field, which is expected to contain information about the gravitational fluctuations in the bulk. We will leave that to future study.

Summary— Every information-preserving RG is dual to a hierarchical generative model. They form the forward and backward pass of the EHM, which is a bijective map between a strongly entangled CFT in flat space-time (boundary) and a weakly entangled bulk field theory in one higher dimension (bulk). The optimal EHM can emerge in the neural network by training a generative model to reproduce the boundary CFT configurations from bulk independent random variables. Previously, the EHM was only designed for free fermion CFT. Using machine learning approaches, we are able to develop more general EHMs that also apply to interacting field theories. This allows us to explore the holographic dual of generic CFTs by learning the effective bulk theory on top of the EHM. At the quadratic order, the effective bulk theory provide us information about the holographic

background geometry. We demonstrated the emergent hyperbolic geometry from a Luttinger liquid CFT in the complex ϕ^4 model. The trained EHM establishes a duality between a gapless CFT on the holographic boundary and a gapped field theory in the holographic bulk, enabling us to study the CFT using our understandings about gapped systems. For example, local updates of the bulk field can be transformed into global updates of the boundary field, which may facilitate the Monte Carlo simulation of gapless systems.

ACKNOWLEDGEMENT

We acknowledge the stimulating discussions with Xiaoliang Qi, John McGreevy, Maciej Koch-Janusz, Wenbo Fu and Shang Liu. S.H.L and L.W. are supported by the National Natural Science Foundation of China under the Grant No. 11774398 and the Strategic Priority Research Program of Chinese Academy of Sciences Grant No. XDB28000000.

* yzyou@physics.ucsd.edu

- [1] E. Witten, *Advances in Theoretical and Mathematical Physics* **2**, 253 (1998), hep-th/9802150.
- [2] E. Witten, *Adv. Theor. Math. Phys.* **2**, 505 (1998), hep-th/9803131.
- [3] S. S. Gubser, I. R. Klebanov, and A. M. Polyakov, *Physics Letters B* **428**, 105 (1998), hep-th/9802109.
- [4] J. Maldacena, *International Journal of Theoretical Physics* **38**, 1113 (1999), hep-th/9711200.
- [5] J. de Boer, E. Verlinde, and H. Verlinde, *Journal of High Energy Physics* **8**, 003 (2000), hep-th/9912012.
- [6] K. Skenderis, *Classical and Quantum Gravity* **19**, 5849 (2002).
- [7] I. Heemskerk and J. Polchinski, *Journal of High Energy Physics* **2011**, 31 (2011), 1010.1264.
- [8] B. Swingle, *ArXiv e-prints* (2012), 1209.3304.
- [9] B. Swingle, *Phys. Rev. D* **86**, 065007 (2012), 0905.1317.
- [10] M. Nozaki, S. Ryu, and T. Takayanagi, *Journal of High Energy Physics* **10**, 193 (2012), 1208.3469.
- [11] V. Balasubramanian, M. Guica, and A. Lawrence, *Journal of High Energy Physics* **1**, 115 (2013), 1211.1729.
- [12] L. P. Kadanoff, *Physics Physique Fizika* **2**, 263 (1966).
- [13] X.-L. Qi, *ArXiv e-prints* (2013), 1309.6282.
- [14] C. H. Lee and X.-L. Qi, *ArXiv e-prints* (2015), 1503.08592.
- [15] Y. Gu, C. H. Lee, X. Wen, G. Y. Cho, S. Ryu, and X.-L. Qi, *ArXiv e-prints* (2016), 1605.00570.
- [16] G. Vidal, *Physical Review Letters* **99**, 220405 (2007), cond-mat/0512165.
- [17] G. Evenbly and G. Vidal, *Physical Review Letters* **112**, 240502 (2014), 1210.1895.
- [18] J. Haegeman, T. J. Osborne, H. Verschelde, and F. Verstraete, *Physical Review Letters* **110**, 100402 (2013), 1102.5524.
- [19] S.-S. Lee, *Journal of High Energy Physics* **1**, 76 (2014), 1305.3908.
- [20] A. Mollabashi, M. Naozaki, S. Ryu, and T. Takayanagi, *Journal of High Energy Physics* **3**, 98 (2014), 1311.6095.
- [21] R. G. Leigh, O. Parrikar, and A. B. Weiss, *Phys. Rev. D* **89**, 106012 (2014), 1402.1430.
- [22] P. Lunts, S. Bhattacharjee, J. Miller, E. Schnetter, Y. B. Kim, and S.-S. Lee, *Journal of High Energy Physics* **8**, 107 (2015), 1503.06474.
- [23] J. Molina-Vilaplana, *ArXiv e-prints* (2015), 1503.07699.
- [24] M. Miyaji, S. Ryu, T. Takayanagi, and X. Wen, *Journal of High Energy Physics* **5**, 152 (2015), 1412.6226.
- [25] X. Wen, G. Y. Cho, P. L. S. Lopes, Y. Gu, X.-L. Qi, and S. Ryu, *ArXiv e-prints* (2016), 1605.07199.
- [26] Y.-Z. You, X.-L. Qi, and C. Xu, *Phys. Rev. B* **93**, 104205 (2016), 1508.03635.
- [27] C. Bény, *ArXiv e-prints* (2013), 1301.3124.
- [28] P. Mehta and D. J. Schwab, *ArXiv e-prints* (2014), 1410.3831.
- [29] D. Oprisa and P. Toth, *ArXiv e-prints* (2017), 1705.11023.
- [30] H. W. Lin, M. Tegmark, and D. Rolnick, *Journal of Statistical Physics* **168**, 1223 (2017), 1608.08225.
- [31] W.-C. Gan and F.-W. Shu, *International Journal of Modern Physics D* **26**, 1743020 (2017), 1705.05750.
- [32] S.-H. Li and L. Wang, *ArXiv e-prints* (2018), 1802.02840.
- [33] M. Koch-Janusz and Z. Ringel, *Nature Physics* **14**, 578 (2018), 1704.06279.
- [34] Y.-Z. You, Z. Yang, and X.-L. Qi, *Phys. Rev. B* **97**, 045153 (2018), 1709.01223.
- [35] K. Hashimoto, S. Sugishita, A. Tanaka, and A. Tomiya, *Phys. Rev. D* **98**, 046019 (2018).
- [36] K. Hashimoto, S. Sugishita, A. Tanaka, and A. Tomiya, *Phys. Rev. D* **98**, 106014 (2018), 1809.10536.
- [37] P. M. Lenggenhager, Z. Ringel, S. D. Huber, and M. Koch-Janusz, *arXiv e-prints arXiv:1809.09632* (2018), 1809.09632.
- [38] P. Olsson, *Phys. Rev. B* **52**, 4526 (1995).
- [39] M. Hasenbusch and K. Pinn, *Journal of Physics A Mathematical General* **30**, 63 (1997), cond-mat/9605019.
- [40] M. Hasenbusch, *Journal of Physics A Mathematical General* **38**, 5869 (2005), cond-mat/0502556.
- [41] D. P. Kingma and M. Welling, *arXiv preprint arXiv:1312.6114* (2013).

SUPPLEMENTARY MATERIAL

A. Minimal Bulk Mutual Information Principle

The maximal real-space mutual information (maxRMI) principle proposed in Ref. 33 and 37 aims to maximize the mutual information between the coarse-grained field and the fine-grained field in the surrounding environment at a single RG step. In this section, we show that the maxRMI principle can be derived from our minimal bulk mutual information (minBMI) principle under certain assumptions.

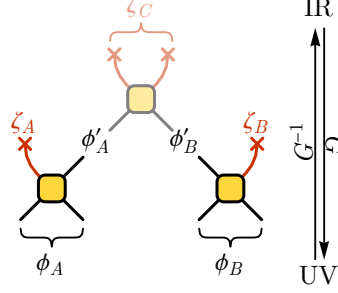


FIG. 6. Functional dependence of variables in the neural-RG network. Each block represents a bijective map.

Let us set up the problem based on Fig. 6. Assuming ϕ_A and ϕ_B are field configurations in two neighboring regions A and B in the UV layer. Under one step of the RG transformation, ϕ_A gets mapped to the coarse grained variable ϕ'_A and the bulk variable ζ_A , and the mapping is bijective. Similarly, another bijection takes ϕ_B to ϕ'_B and ζ_B . Eventually, ϕ'_A and ϕ'_B will be mapped to the bulk field ζ_C in deeper IR layers. Therefore the random variables appeared in Fig. 6 are related by the following bijections f_A, f_B, f_C as

$$(\phi'_A, \zeta_A) = f_A(\phi_A), (\phi'_B, \zeta_B) = f_B(\phi_B), \zeta_C = f_C(\phi'_A, \phi'_B). \quad (13)$$

What are the information theoretical principles to guide the bijections f_A, f_B, f_C toward good RG transformations? We propose the minBMI principle that these bijections should minimize the mutual information among the bulk variables,

$$\min I(\zeta_A : \zeta_B) + I(\zeta_A : \zeta_C) + I(\zeta_B : \zeta_C). \quad (14)$$

Ref. 33 and 37 propose another principle, the maxRMI principle, that the RG transformation should maximize the mutual information between the coarse grained variable (such as ϕ'_A) and its environments (such as ϕ_B),

$$\max I(\phi'_A : \phi_B). \quad (15)$$

We can show that the objective of the maxRMI in Eq. (15) is consistent with the objective of the minBMI in Eq. (14) in the limit of UV-IR decoupling.

The minBMI principle aims to minimize mutual information among all bulk variables, both between different RG scales and within the same RG scale. Its objective has a broader scope than the maxRMI principle, because the later does not specify its objectives across the RG scales. So to make a connection between these two principles, one must first restrict the scope of the minBMI principle to a single layer. This can be achieved by assuming that there is no mutual information between bulk variables at different RG scales. In our setup, this corresponds to $I(\zeta_A, \zeta_B : \zeta_C) = 0$, which factorizes the joint probability $p(\zeta_A, \zeta_B, \zeta_C) = p(\zeta_A, \zeta_B)p(\zeta_C)$ and decouples the bulk variables between UV and IR. As a result, the mutual information between any bulk variables across different RG scales vanishes $I(\zeta_A : \zeta_C) = I(\zeta_B : \zeta_C) = 0$. This already minimizes the bulk mutual information across layers and reduces the minBMI objective in Eq. (14) to

$$\min I(\zeta_A : \zeta_B). \quad (16)$$

In this UV-IR decoupled limit, we can prove that $\max I(\phi'_A : \phi_B)$ and $\min I(\zeta_A : \zeta_B)$ are equivalent.

The proof starts by considering the mutual information between ϕ_A and ϕ_B . We can see that

$$\begin{aligned}
 I(\phi_A : \phi_B) &= I(\phi'_A, \zeta_A : \phi_B) \\
 &= I(\phi'_A : \phi_B) + I(\zeta_A : \phi_B) \\
 &= I(\phi'_A : \phi_B) + I(\zeta_A : \phi'_B, \zeta_B) \\
 &= I(\phi'_A : \phi_B) + I(\zeta_A : \phi'_B) + I(\zeta_A : \zeta_B) \\
 &= I(\phi'_A : \phi_B) + I(\zeta_A : \zeta_B).
 \end{aligned} \tag{17}$$

Here we have used the bijective property of f_A, f_B, f_C to obtain $I(\phi_A : \phi_B) = I(\phi'_A, \zeta_A : \phi_B)$, $I(\zeta_A : \phi_B) = I(\zeta_A : \phi'_B, \zeta_B)$ and $I(\zeta_A : \zeta_C) = I(\zeta_A : \phi'_A, \phi'_B)$. In the UV-IR decoupled limit, $I(\zeta_A : \zeta_C) = 0$, so $I(\zeta_A : \phi'_A, \phi'_B) = 0$, which further implies $I(\zeta_A : \phi'_A) = I(\zeta_A : \phi'_B) = 0$. With these relations, all steps in Eq. (17) are justified. On the left hand side, $I(\phi_A : \phi_B)$ is determined by the field theory in the UV layer, which can be treated as a constant. For the given amount of information between regions A and B , Eq. (17) tells us that $I(\phi'_A : \phi_B)$ and $I(\zeta_A : \zeta_B)$ are competing for information resources. Therefore maximizing $I(\phi'_A : \phi_B)$ is equivalent to minimizing $I(\zeta_A : \zeta_B)$.

We can apply this argument layer by layer. Then to achieve the objective of the maxRMI principle, we need to minimize mutual information among bulk variables in the same RG scale, which is precisely the statement of the minBMI principle when restricted to each layer. In this sense, the maxRMI and minBMI principles are consistent. However, the minBMI principle actually relaxes the assumption that bulk variables at different RG scales are fully decoupled. Instead, we want to minimize mutual information among all bulk variables, including those across the scales. In this sense, the minBMI principle is more general than the maxRMI principle.

B. Bulk field theory design

In finding the effective bulk field theory, we assume the bulk field is very massive. Under this assumption, higher-order interaction terms are irrelevant. Therefore, we use a correlated Gaussian distribution with positive definite kernel matrix K as our effective bulk field theory. We also assumed locality of our effective bulk field theory, which means K_{ij} is non-zero if and only if ζ_i and ζ_j are nearest neighbors in the bulk, including neighbors inter-scale and intra-scale. To further reduce the fitting parameters of matrix K , we also imposed translation invariance of the bulk field at each scale. This is reasonable, because our RG scheme also has the translation invariance at each scale.

To ensure matrix K is positive definite, we decomposed matrix K into a set of positive semi-definite matrix and a mass term. Particularly,

$$K = \sum_{\langle ij \rangle} \lambda_{ij} (|i\rangle\langle i| + |j\rangle\langle j| - |i\rangle\langle j| - |j\rangle\langle i|) + m\mathbb{I}, \tag{18}$$

where \mathbb{I} is the identity matrix, and λ_{ij} and m are positive numbers. This ensures matrix K we constructed is positive definite.

C. Hyperbolic space

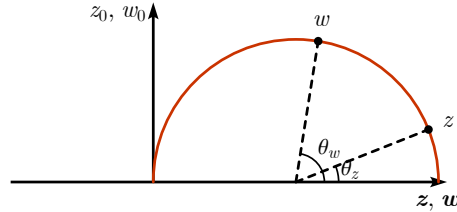


FIG. 7. Geodesic distance in hyperbolic space.

The metric of Euclidean AdS_{d+1} space (the hyperbolic space) is given by

$$ds^2 = g_{\mu\nu} dz^\mu dz^\nu = \frac{1}{z_0^2} (dz_0 dz_0 + \mathbf{dz} \cdot \mathbf{dz}) \quad (19)$$

The geodesic equation is given by

$$\begin{aligned} \frac{d^2 z_0}{d\tau} - \frac{1}{z_0} \left(\frac{dz_0}{d\tau} \right)^2 + \frac{1}{z_0} \left(\frac{d\mathbf{z}}{d\tau} \right)^2 &= 0, \\ \frac{d^2 \mathbf{z}}{d\tau} - \frac{2}{z_0} \frac{dz_0}{d\tau} \frac{d\mathbf{z}}{d\tau} &= 0. \end{aligned} \quad (20)$$

As shown in Fig. 7, given any two points z and w in hyperbolic space, there is a unique semi-circle connecting them. The geodesic distance can be calculated as

$$d(z|w) = \text{arccosh} \frac{z_0^2 + w_0^2 + (\mathbf{z} - \mathbf{w})^2}{2z_0 w_0}. \quad (21)$$

The ideal distance matrix in Fig. 5 is generated using (21).

D. Design of bijectors

We designed a set of symmetry-persevere bijectors to making sure that $U(1)$ symmetry of the boundary is preserved at each bijector. For the generative process, at each RG step, it takes the four complex degrees of freedom and they go through three layers of bijectors: \mathcal{S} , \mathcal{O} , and \mathcal{A} .

I. Scaling layer(\mathcal{S}): At scaling layer, each complex variables ϕ_i is multiplied by a factor e^{λ_i} . The inverse and the Jacobian of this transformation can be obtained easily.

II. Orthogonal transformation layer(\mathcal{O}): The orthogonal transformation in disentangler and decimator is in general an $O(4)$ transformation. In stead, we implemented it by stacking multiple $O(2)$ transformations. In Fig. 8(a), each blue block represents the matrix:

$$M_{\text{blue}}(\theta_i) = \begin{pmatrix} \sin \theta_i & \cos \theta_i \\ \cos \theta_i & -\sin \theta_i \end{pmatrix}, \quad (22)$$

and the orange block in Fig. 8(b) represents the matrix:

$$M_{\text{orange}}(\theta_i) = \begin{pmatrix} \cos \theta_i & -\sin \theta_i \\ \sin \theta_i & \cos \theta_i \end{pmatrix}. \quad (23)$$

θ_i in those blocks are training parameters. The arrangement of the type I and type II blocks are such designed that when $M_{\text{blue}}(\theta_i = \pi/4)$ and $M_{\text{orange}}(\theta_i = 0)$ the network reproduces the ideal EHM originally proposed in Ref. 13. We initialize the parameter to this ideal limit.

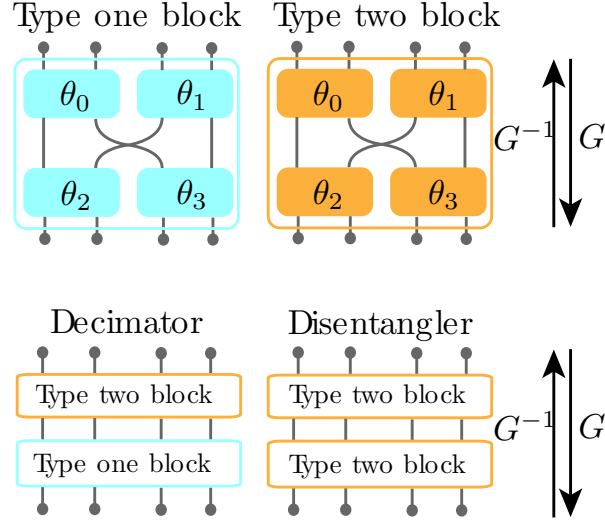


FIG. 8. Orthogonal transformation.

III. Non-linear layer(\mathcal{A}) For non-linear part, we use the amplitude hyperbolic functions for complex field ϕ_i . In coarse-graining direction, it acts in the following,

$$\begin{aligned} \text{Re}(\zeta) &= \sinh |\phi| \frac{\text{Re } \phi}{|\phi|}; \\ \text{Im}(\zeta) &= \sinh |\phi| \frac{\text{Im } \phi}{|\phi|}. \end{aligned} \tag{24}$$

The corresponding inverse and Jacobian can be calculated easily.